APPLIED AND ENVIRONMENTAL MICROBIOLOGY, Nov. 2002, p. 5585–5594 Vol. 68, No. 11
0099-2240/02/$04.00+0 DOI: 10.1128/AEM.68.11.5585–5594.2002

MtrB Is Required for Proper Incorporation of the Cytochromes OmcA and OmcB into the Outer Membrane of *Shewanella putrefaciens* MR-1

Charles R. Myers* and Judith M. Myers

Department of Pharmacology and Toxicology, Medical College of Wisconsin, Milwaukee, Wisconsin 53226

Received 14 May 2002/Accepted 5 August 2002

When grown under anaerobic conditions, *Shewanella putrefaciens* MR-1 synthesizes multiple outer membrane (OM) cytochromes, some of which have a role in the use of insoluble electron acceptors (e.g., MnO_2) for anaerobic respiration. The cytochromes OmcA and OmcB are localized to the OM and the OM-like intermediate-density membrane (IM) in MR-1. The components necessary for proper localization of these cytochromes to the OM have not been identified. A gene replacement mutant (strain MTRB1) lacking the putative OM protein MtrB was isolated and characterized. The specific cytochrome content of the OM of MTRB1 was only 36% that of MR-1. This was not the result of a general decline in cytochrome content, however, because the cytoplasmic membrane (CM) and soluble fractions were not cytochrome deficient. While OmcA and OmcB were detected in the OM and IM fractions of MTRB1, significant amounts were mislocalized to the CM. OmcA was also detected in the soluble fraction of MTRB1. While OmcA and OmcB in MR-1 fractions were resistant to solubilization with Triton X-100 in the presence of Mg^{2+}, Triton X-100 readily solubilized these proteins from all subcellular fractions of MTRB1. Together, these data suggest that MtrB is required for the proper localization and insertion of OmcA and OmcB into the OM of MR-1. The inability of MTRB1 to properly insert these, and possibly other, proteins into its OM likely contributes to its marked deficiency in manganese(IV) and iron(III) reduction. While the localization of another putative OM cytochrome (MtrF) could not be directly determined, an *mtrF* gene replacement mutant exhibited wild-types rates of Mn(IV) and Fe(III) reduction. Therefore, even if MtrF were mislocalized in MTRB1, it would not contribute to the loss of metal reduction activity in this strain.

Shewanella putrefaciens MR-1 can use a wide variety of terminal electron acceptors for anaerobic respiration, including insoluble manganese (Mn) and iron (Fe) oxides (17, 19, 23, 24, 26). MR-1 and other strains of *Shewanella* may contribute to the reductive solubilization of metal oxides in various environments and may be useful in the remediation of certain metal-contaminated sites.

Understanding the mechanisms by which bacteria generate energy from the reduction of insoluble electron acceptors [e.g., Fe(III) and Mn(IV) oxides] should contribute to a better understanding of bacterial anaerobic respiration and of the reduction of metals in various environments. Various cytochromes in MR-1 have roles in metal reduction (20, 21, 25–27). When grown under anaerobic conditions, MR-1 localizes a majority of its membrane-bound cytochromes to the outer membrane (OM) (15). All of its OM cytochromes contain *c*-type hemes (21). Two of these OM cytochromes, OmcA and OmcB, have been purified, and sequence analyses have predicted that both are lipoproteins and contain 10 consensus heme *c*-binding domains (CXXCH) (21, 25, 27). These cytochromes are localized in the OM, where they could potentially make direct contact with extracellular metal oxides at the cell surface and therefore could represent a link between the electron transport systems and the reduction of extracellular insoluble metal oxides.

Mutants with interrupted *omcA* and *omcB* genes have partial and prominent deficiencies in Mn(IV) reduction, respectively (27). *omcB* mutants are also compromised in terms of Fe(III) citrate reduction, especially when they are compared to the wild type after 24 h or less (3, 28). However, the *omcB* mutant OMCB1 is capable of significant reduction of Fe(III) citrate, with >4 mM Fe(II) generated after 5 days (28). Fe(III) citrate reduction can be fully restored and amorphous ferric oxyhydroxide (αFeOOH) reduction can be partially restored to OMCB1 without restoration of OmcB (28). This suggests that OmcB is not necessary for Fe(III) reduction.

Two genes immediately downstream from *omcB*, *mtrA* and *mtrB*, encode proteins with putative roles in Mn(IV) and Fe(III) reduction (2, 3). Some evidence suggests that *omcB*, *mtrA*, and *mtrB* are transcribed as a polycistronic mRNA (3). However, reverse transcription-PCR analysis has demonstrated that *mtrA-mtrB* mRNA is present in the *omcB* mutant OMCB1 (28). MtrA is a periplasmic *c*-type cytochrome (3) which could potentially serve as an electron carrier, but it is not localized where it could directly transfer electrons to extracellular insoluble metal oxides. MtrB has been putatively localized to the OM on the basis of Sarkosyl insolubility (2), but it does not have any obvious electron transport moieties so its role in metal reduction is unclear.

To better understand the role of MtrB in metal reduction, studies with an *mtrB* gene replacement mutant revealed that

* Corresponding author. Mailing address: Department of Pharmacology and Toxicology, Medical College of Wisconsin, 8701 Watertown Plank Road, Milwaukee, WI 53226. Phone: (414) 456-8593. Fax: (414) 456-6545. E-mail: cmyers@mcw.edu.

TABLE 1. Bacteria and plasmids used in this study

Bacterial strain or plasmid	Description[a]	Reference	Source
S. putrefaciens strains			
MR-1	Manganese-reducing strain from Lake Oneida, N.Y., sediments	23	Previous study
MTRB1	*mtrB* mutant derived from MR-1; *mtrB*::Km^r		This study
MTRF1	*mtrF* mutant derived from MR-1; *mtrF*::Km^r		This study
MTRF-OMCA	*mtrF-omcA* mutant derived from MR-1; *mtrF*::Km^r::*omcA*		This study
E. coli strains			
S17-1λ *pir*	λ(*pir*) *hsdR pro thi,* chromosomal integrated RP4-2 Tc::Mu Km::Tn*7;* donor strain used to mate pEP185.2-derived plasmids into MR-1	36	V. L. Miller
TOP10	F$^-$ *mcrA* Δ(*mrr-hsdRMS-mcrBC*) ϕ80*lacZ*ΔM15 Δ*lacX74 deoR recA1 araD139* Δ(*ara-leu*)*7697 galU galK rpsL* (Sm^r) *endA1 nupG;* used as host for plasmids derived from pCR2.1-TOPO and pBAD/Thio-TOPO		Invitrogen
Plasmids			
pBAD/Thio-TOPO	4.4-kb vector for generating MtrB antigen fusion; Ap^r		Invitrogen
pCR2.1-TOPO	3.9-kb vector for cloning PCR products; Ap^r		Invitrogen
pEP185.2	4.28-kb mobilizable suicide vector derived from pEP184; *oriR6K mobRP4* Cm^r	11	V. L. Miller
pEPsacB	Mobilizable suicide vector derived from pEP185.2; *sacB* cloned into the *Nsi*I site of PEP185.2	27	Previous study
pUT/mini-Tn*5Km*	Ap^r; Tn*5*-based delivery plasmid; used as source of Km^r gene	6	D. Frank
pTOPO/mtrB	pCR2.1-TOPO with *mtrB* plus associated 5′ and 3′ DNA from MR-1; 6.2 kb		This study
pTOPO/mtrF	pCR2.1-TOPO with *mtrF* plus associated 5′ and 3′ DNA from MR-1; 6.1 kb		This study
pTOPO/mtrF-omcA	pCR2.1-TOPO with *mtrF* and *omcA* plus associated 5′ and 3′ DNA from MR-1; 8.4 kb		This study
pTOPO/mtrB:Km	pTOPO/mtrB with the Km^r gene replacing 868 bp of *mtrB;* 7.4 kb		This study
pTOPO/mtrF:Km	pTOPO/mtrF with the Km^r gene replacing 492 bp of *mtrF*		This study
pTOPO/mtrF:Km:omcA	pTOPO/mtrF-omcA with the Km^r gene replacing a 2,492-bp fragment spanning *mtrF* and *omcA*		This study
pDSEP/mtrB:Km	Km^r gene-interrupted *mtrB* gene from pTOPO/mtrB:Km cloned into the *Eco*RV site of pEP185.2; Cm^r Km^r; used for gene replacement to generate MTRB1		This study
pDSEPsac/mtrF:Km	Km^r gene-interrupted *mtrF* gene from pTOPO/mtrF:Km cloned into the *Xho*I site of pEPsacB; Cm^r Km^r; used for gene replacement to generate MTRF1		This study
pDSEP/mtrF:Km:omcA	Km^r gene-interrupted *mtrF-omcA* fragment from pTOPO/mtrF:Km:omcA cloned into the *Eco*RV site of pEP185.2; Cm^r Km^r; used for gene replacement to generate MTRF-OMCA		This study

[a] Km^r, Ap^r, Cm^r, and Sm^r, resistance to kanamycin, ampicillin, chloramphenicol, and streptomycin, respectively.

MtrB is necessary for proper incorporation of the cytochromes OmcA and OmcB into the OM of MR-1. This has important implications for the deficiency in metal reduction associated with the loss of MtrB.

MATERIALS AND METHODS

All chemicals, enzymes, and other reagents were obtained from previously described sources (20, 26), unless indicated otherwise below.

Bacterial strains, plasmids, media, and growth conditions. A list of the bacteria and plasmids used in this study is presented in Table 1. For molecular biology purposes, *S. putrefaciens* and *Escherichia coli* were grown aerobically on Luria-Bertani medium (33) supplemented, when required, with antibiotics at the following concentrations: ampicillin, 50 μg ml^{-1}; kanamycin, 50 μg ml^{-1}; and chloramphenicol, 34 μg ml^{-1}. *E. coli* was grown at 37°C, whereas *S. putrefaciens* was grown either at 30°C or at room temperature (23 to 25°C).

For preparation of subcellular fractions, *S. putrefaciens* was grown under anaerobic conditions as previously described (15) in M1 defined medium (24) supplemented with 15 mM lactate, 24 mM fumarate, and vitamin-free Casamino Acids (0.2 g liter^{-1}). For testing of Mn(IV) or Fe(III) reduction, the defined medium was similarly supplemented with vitamin-free Casamino Acids,15 mM lactate, and 15 mM formate plus either 4.5 mM vernadite (δMnO_2), 10 mM ferric citrate, or 2 mM αFeOOH. For testing of Mn(IV) and Fe(III) reduction or growth on other electron acceptors, inocula were prepared by using cells grown aerobically for 1 day on Luria-Bertani medium supplemented with the appropriate antibiotics; the cells were suspended in sterile distilled water, and the inoculum densities were adjusted to equalize the turbidity (optical density at 500 nm, as determined with a Beckman DU-64 spectrophotometer). For testing of anaerobic growth, the medium was supplemented with one of the following electron acceptors, as indicated below: 20 mM fumarate, 2 mM nitrate, or 5 mM dimethyl sulfoxide (DMSO).

DNA manipulations. A list of the synthetic oligonucleotides used in this study is presented in Table 2. Restriction digestion, mapping, cloning, subcloning, and DNA electrophoresis were performed by using standard techniques (33) and by following the manufacturers' recommendations as appropriate. The following procedures were performed as previously reported (27): DNA ligation, isolation of plasmid DNA, colony PCR, and determination of the sizes of DNA fragments

TABLE 2. Synthetic oligonucleotides used in this study

Oligonucleotide	Sequence[a]
RB1	5′-TGCTCGAGCAGCAACGCCTACTTAG-3′
RB2	5′-TGCTCGAGATATTTGTGCGCTATTGAGACTC-3′
RB3	5′-TGCTCGAGTATGAGGCAAATGGATTAGAG-3′
RB4	5′-TGCTCGAGGCGGTCGCTTAGATGT-3′
RB5	5′-GCTGATGGTTATGGTCTAGCGAATG-3′
RB6	5′-TGCGGTGTAGTCATGGCTGTTACT-3′
F1	5′-TGCTCGAGTACGGTTCGATTGGCTATTTGAG-3′
F2	5′-TGCTCGAGCTTTAAGCGGGTAATGTGATTGA-3′
F3	5′-TTGGCGCGCCTGAGCCTAACCAACCCAACCACA-3′
F4	5′-TTGGCGCGCCTGAGGACTGCCAATCATAATGTT-3′
F5	5′-GGCACTGGCGTCGTCTATC-3′
F6	5′-TTTGTTGCGGTATTGAAATTGAAC-3′
F7	5′-TTGGCGCGCCAAGCGTTGGGTGGCATCACTTAG-3′
A2	5′-TGCTCGAGAAGATACCGCCGTTAGTTTC-3′
A4	5′-TTGGCGCGCCAGTGTCGCATTTATTGGCAGA-3′
A7	5′-TGGGCGCGCCATCCAGAATCAGGCAATAGCATT-3′
K1	5′-ATTGCGATCGATTTATGCTTGTAAACCGTT-3′
AK1	5′-TTGGCGCGCCTTATGCTTGTAAACCGTT-3′

[a] The underlined regions indicate the following restriction endonuclease sites engineered into the oligonucleotides: *Xho*I sites in RB1, RB2, RB3, RB4, F1, F2, and A2; *Asc*I sites in F3, F4, F7, A7, and AK1; and a *Cla*I site in K1.

and proteins. Computer-assisted sequence analysis and comparisons were performed by using MacVector software (Accelrys, San Diego, Calif.). Oligonucleotide primers were designed by using OLIGO primer analysis software (version 6.15; Molecular Biology Insights, Cascade, Colo.).

Electroporation and preparation of cells for electroporation were performed as previously described (20, 27).

Construction of *mtrB* gene replacement mutant. An *mtrB* gene replacement mutant (MTRB1) was constructed from MR-1 by using a strategy analogous to that previously used to construct mutants with mutations in *omcA, omcB*, and *cymA* (26, 27). A 2.3-kb fragment containing the entire *mtrB* gene plus 5′ and 3′ flanking sequences was generated by PCR amplification of MR-1 genomic DNA with primers RB1 and RB2. The PCR product was cloned into pCR2.1-TOPO, which generated pTOPO/mtrB. pTOPO/mtrB was digested with *Cla*I, which yielded an 868-bp internal fragment of *mtrB* and a 5.3-kb fragment (TOPO/mtrBΔ868). The 2.1-kb Km^r gene from pUT/mini-Tn*5Km* was generated by PCR with primer K1. Following digestion with *Cla*I, the Km^r gene was ligated to the 5.3-kb TOPO/mtrBΔ868 fragment, which generated pTOPO/mtrB:Km. A 3.1-kb DNA fragment containing the Km^r gene flanked by regions of *mtrB* was generated by PCR by using pTOPO/mtrB:Km as the template and primers RB3 and RB4. This fragment was blunt ended and ligated into the *Eco*RV site of the suicide vector pEP185.2, which generated pDSEP/mtrB:Km. *E. coli* S17-1λpir(pDSEP/mtrB:Km) was mated with MR-1, and kanamycin-resistant MR-1 exconjugants were selected under aerobic conditions on M1 defined medium with 15 mM lactate as the electron donor. Colonies were screened by colony PCR to identify clones with interrupted *mtrB*. Throughout this procedure, appropriate analyses (e.g., restriction digestion and PCR) were done to verify that the expected constructs were obtained.

Construction of *mtrF and mtrF-omcA* gene replacement mutants. An *mtrF* gene replacement mutant (MTRF1) and an *mtrF-omcA* double mutant (MTRF-OMCA) were constructed from MR-1 by using similar strategies.

For the *mtrF* mutant, primers F1 and F2 were used to amplify *mtrF* plus flanking DNA from MR-1 genomic DNA; ligation into pCR2.1-TOPO generated pTOPO/mtrF. Inverse PCR (29) was performed by using pTOPO/mtrF and primers F3 and F4 and generated TOPO/mtrF(Δ492), a linear fragment that is missing 492 bp of internal *mtrF* sequence. Following digestion with *Asc*I, TOPO/mtrF(Δ492) was ligated to the *Asc*I-digested Km^r gene, which had been amplified from pUT/mini-Tn*5Km* by using primer AK1. The Km^r-interrupted *mtrF* gene was excised from the resulting construct (pTOPO/mtrF:Km) and was ligated into the *Xho*I site of pEPsacB, which generated pDSEPsac/mtrF:Km. *E. coli* S17-11pir(pDSEPsac/mtrF:Km) was mated with MR-1, and kanamycin-resistant MR-1 exconjugants were screened by colony PCR by using primers F5 and F6.

For the *mtrF-omcA* double mutant, primers F1 and A2 were used to amplify a 4.5-kb fragment from MR-1 genomic DNA that contained all of *mtrF* plus upstream DNA and most of *omcA*; ligation into pCR2.1-TOPO generated pTOPO/mtrF-omcA. Inverse PCR was performed by using pTOPO/mtrF-omcA and primers F7 and A7 and generated TOPO/mtrF-omcA(Δ2492), a linear fragment that is missing 2,492 bp, including 1,465 bp of the 3′ end of *mtrF* and 778 bp of the 5′ end of *omcA*. *Asc*I-cut TOPO/mtrF-omcA(Δ2492) was ligated to the *Asc*I-digested Km^r gene (see above). From the resulting construct (pTOPO/mtrF:Km:omcA), the *mtrF*:Km^r:*omcA* fragment was amplified by PCR by using primers F1 and A2. This fragment was blunt ended and ligated into the *Eco*RV site of the suicide vector pEP185.2, which generated pDSEP/mtrF:Km:omcA. *E. coli* S17-1λpir(pDSEP/mtrF:Km:omcA) was mated with MR-1, and kanamycin-resistant MR-1 exconjugants were screened by colony PCR by using primers F1 and A2.

Purification and characterization of subcellular fractions. Cytoplasmic membrane (CM), intermediate membrane (IM), OM, and soluble fractions (periplasm plus cytoplasm) were purified from cells by using an EDTA-lysozyme-Brij protocol as previously described (15). IM fractions have also been observed during subcellular fractionation of other gram-negative bacteria. Except for a buoyant density intermediate the between the buoyant densities of the CM and OM, the IM closely resembles the OM (21). The separation and purity of these subcellular fractions were assessed by using spectral cytochrome content (15), membrane buoyant density (15), and NADH oxidase activity (30) as indicated below. Sodium dodecyl sulfate (SDS)-polyacrylamide gel electrophoresis (PAGE) gels (25) were stained for protein with Pro-Blue (Owl Separation Systems, Woburn, Mass.) or for heme (37).

Triton X-100 solubility of membrane cytochromes. The ability of Triton X-100 to solubilize cytochromes from various membrane fractions was examined by using an extraction protocol (10, 34) designed to selectively solubilize CM components (15). Membrane fractions (0.75 mg of protein) were suspended in 1.0 ml of 10 mM HEPES (pH 7.5)–10 mM $MgCl_2$ and incubated overnight at 4°C. The fractions were equilibrated to room temperature, and Triton X-100 (Aldrich Chemical) was added to a final concentration of 2.0% (vol/vol). The controls included identical samples with no Triton X-100. Following incubation for 10 min at room temperature, 1.0 ml of cold 10 mM HEPES (pH 7.5) was added, and the Triton X-100-insoluble material was pelleted by ultracentrifugation (38,000 rpm, 128,600 × *g*, 2 h, 4°C, Beckman 50.3Ti rotor). The resulting pellets were suspended in 0.6 ml of 10 mM HEPES (pH 7.5), and the suspensions were analyzed spectrally for cytochrome content (15).

Antibody specific for MtrB. Recombinant technology was used to generate a protein fusion of thioredoxin (TR) to an internal 665-residue fragment of MtrB. Specifically, a 1,995-bp fragment of *mtrB* was generated by PCR amplification of MR-1 genomic DNA with custom primers RB5 and RB6. This PCR product was cloned into pBAD/Thio-TOPO (Invitrogen, Carlsbad, Calif.) and transformed into *E. coli* TOP10. After a clone in which the *mtrB* insert was in the proper orientation was identified, expression of the fusion protein was induced with 0.02% arabinose for 2 h at 37°C. The cells were harvested by centrifugation and lysed with Bugbuster protein extraction reagent (Novagen, Madison, Wis.). The resulting fusion protein, which contained the 665-residue fragment of MtrB sandwiched between TR at the N terminus and a six-histidine tag at the C terminus, was localized primarily in inclusion bodies. After solubilization with 6 M urea, the TR-MtrB fusion was purified by using His-Bind Quick resin (Novagen) according to the manufacturer's instructions. The purified fusion protein was concentrated by ultrafiltration and then dialyzed at 4°C against 20 mM Tris-HCl (pH 7.4)–50 mM NaCl. The dialyzed TR-MtrB fusion protein was used as an antigen to generate polyconal antisera in New Zealand White rabbits as previously described (21), except that Titermax (CytRx Corp., Norcross, Ga.) was used as an adjuvant.

Miscellaneous procedures. The polyclonal antibodies specific for OmcA and OmcB were the polyclonal antibodies described in a previous study (28). Purification of immunoglobulin G (IgG) from rabbit sera, removal of nonspecific antibodies by absorption with *E. coli,* and Western blotting were performed as previously described (21), except that the following changes were made to the Western blotting protocol: (i) the samples were boiled for 5 min in SDS solubilization mixture (25) buffer prior to SDS-PAGE; (ii) the resolved proteins were transferred to a nitrocellulose membrane for 1 h at 0.4 A (Hoefer TE22 Transphor unit; Hoefer Pharmacia Biotech, Piscataway, N.J.); (iii) the primary antibodies (final purified IgG concentration in blocking solution, 1 μg ml^{-1}) were incubated with the blots for 90 min; (iv) the secondary antibody was goat anti-rabbit Ig–horseradish peroxidase (BD Transduction Laboratories, Lexington, Ky.) used at a final concentration of 33.3 ng ml^{-1} in blocking solution; (v) after removal of the secondary antibody, the blots were washed six times; and (vi) the blots were developed with a SuperSignal West Pico kit (Pierce, Inc., Rockford, Ill.). The anti-MtrB IgG was not preadsorbed with *E. coli* cells because this removed anti-MtrB.

Mn(II) contents in filtrates were determined by a formaldoxime method (1, 4). δMnO_2 (23) and αFeOOH (12) were prepared as described previously. Fe(II) contents were determined by a ferrozine extraction procedure (12, 22). Nitrate (5) and nitrite (39) contents were determined colorimetrically by using cell-free filtrates. Growth was assessed by measuring culture turbidity at 500 nm with a Beckman DU-64 spectrophotometer. Protein contents were determined by a modified Lowry method by using bovine serum albumin as the standard (20).

Statistical analysis was performed by using analysis of variance and Tukey's multiple comparison posttest (InStat software; GraphPad, San Diego, Calif.).

RESULTS

The linear arrangement of the genes and open reading frames in the MR-1 genome from *mtrF* downstream is shown in Fig. 1. The *omcA* and *omcB* genes encode decaheme *c*-type cytochromes which are putative OM lipoproteins that have roles in metal reduction (25, 27, 28). *mtrF* also encodes a putative decaheme *c*-type cytochrome with a lipoprotein consensus sequence (LXXC) (9) located at residues 21 to 24 of the immature protein. Based on these similarities to OmcA and OmcB, we predict that MtrF could be another OM cytochrome.

Metal reduction and cytochrome distribution in the *mtrB* mutant. Strain MTRB1 lacked the expected wild-type PCR product for *mtrB* but was positive for a PCR product that was ~1.2 kb larger (Fig. 2), which was consistent with replacement

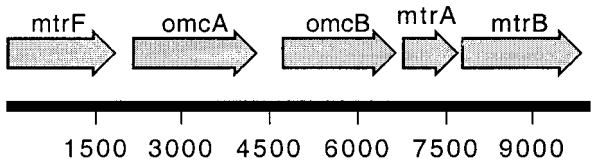

FIG. 1. Linear orientation of the gene cluster of MR-1 from *mtrF* downstream to beyond the 3′ end of *mtrB*, as derived from the preliminary genomic sequence data provided by The Institute for Genomic Research (http://www.tigr.org). The diagram is drawn to scale, and the transcription direction for all genes is from left to right (5′ → 3′).

of 0.87 kb of *mtrB* with the ~2.1-kb Km^r gene. MTRB1 was positive for the PCR product (with primer K1) expected for the Km^r gene used to interrupt *mtrB* but was unable to grow on medium containing chloramphenicol. Overall, these results are consistent with double-crossover gene replacement of *mtrB*, as single-crossover insertion into the genome should have retained the *cat* gene of the suicide vector pEP185.2.

Compared to the wild type, MTRB1 was markedly deficient in the reduction of Mn(IV) (Fig. 3) and Fe(III) citrate (data not shown). The levels of Mn(II) generated by MTRB1 were statistically the same as those in the sterile control (blank) (Fig. 3). The levels of Fe(II) generated by MTRB1 were also very low, although they were statistically greater than those in the sterile control at 48 and 72 h ($P < 0.01$) (data not shown). These deficiencies in Mn(IV) and Fe(III) reduction do not reflect a pleiotropic deficiency in anaerobic electron acceptor use, because the anaerobic growth of MTRB1 on fumarate and DMSO was very similar to that of MR-1 (i.e., both strains reached essentially the same maximal culture turbidity after 24 h) (data not shown). Both strains also reduced 2 mM nitrate to undetectable levels by 24 h; nitrite was not detected at 24 h, indicating that nitrite was also rapidly reduced (data not shown).

When grown under anaerobic conditions, MR-1 localizes a majority of its membrane-bound cytochromes to the OM (15); all of the OM cytochromes contain *c*-type hemes (21). However, when examined quantitatively, the specific cytochrome content of the OM of MTRB1 was only 36% that of MR-1 (Fig. 4). Similarly, the specific cytochrome content of the IM of MTRB1 was 37% that of MR-1. The IM of MR-1 closely resembles the OM in many respects (21) and may consist largely of OM fragments with a lower buoyant density. The lower cytochrome content of the IM and OM of MTRB1 is not indicative of a general decline in cytochrome content, however, as the specific cytochrome contents of the soluble fractions of the two strains were essentially identical. While the CM of MTRB1 had a marginally higher cytochrome content than the CM of the wild type, the differences were not statistically significant (Fig. 4). The SDS-PAGE protein profiles of the various subcellular fractions showed that the overall protein pattern in the IM and OM of MTRB1 was similar to that of MR-1 (Fig. 5), so the differences in OM cytochrome content do not represent global changes in OM composition. There were some additional high-molecular-weight bands present in the CM of MTRB1 that were not present in the CM of MR-1 (Fig. 5), which could represent OM cytochromes mislocalized to the CM (see below).

Since OmcA and OmcB have a role in Mn(IV) reduction (27, 28), a decline in OM cytochrome content should result in a decline in Mn(IV) reduction. MTRB1 had lost essentially all Mn(IV) reduction activity (Fig. 3) and approximately two-thirds of the specific OM cytochrome content (Fig. 4). This suggested the possibility that the insertion or configuration of the remaining OM cytochromes in MTRB1 was not optimal. This possibility was examined by using a differential detergent extraction protocol. In the presence of Mg^{2+}, the nonionic detergent Triton X-100 can solubilize most cytochromes from the CM of MR-1, whereas cytochromes in the IM and OM

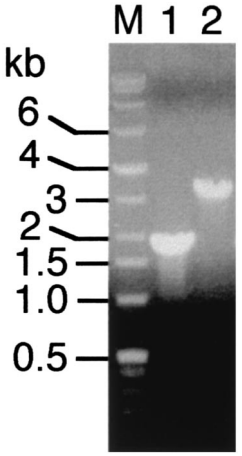

FIG. 2. Colony PCR for MR-1 (lane 1) and MTRB1 (lane 2) performed with primers RB3 and RB4 specific for the *mtrB* gene. The sizes of the DNA markers (lane M) are indicated on the left.

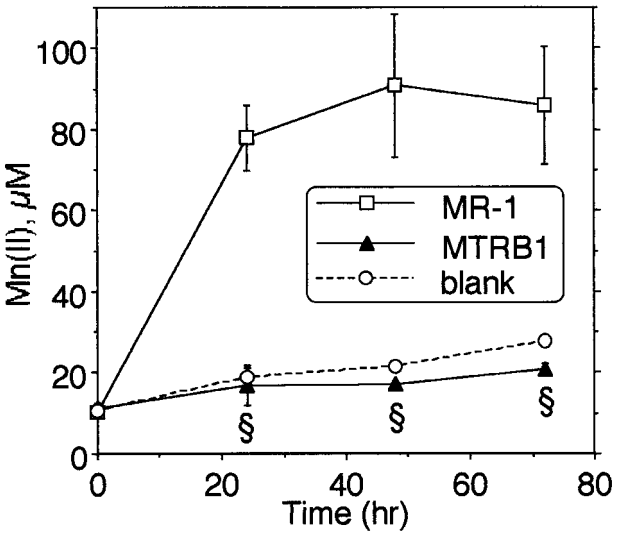

FIG. 3. Reduction of δMnO_2 by MR-1 and MTRB1 cells under anaerobic conditions as determined by the formation of Mn(II) over time. All values are means ± standard deviations for three independent cultures of each strain. For points lacking error bars, the bars were smaller than the symbols. A section sign indicates that the value for MTRB1 was statistically significantly different from the value for MR-1 at a *P* value of <0.001. The values for MTRB1 were similar to those for the blank ($P > 0.05$).

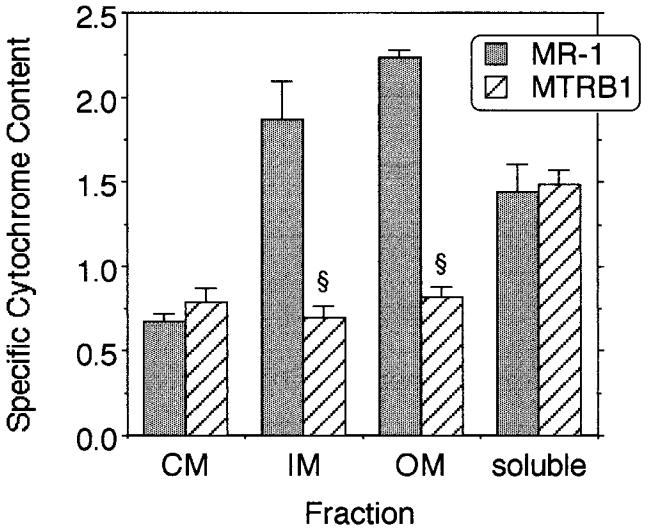

FIG. 4. Specific cytochrome contents of the subcellular fractions prepared from strains MR-1 and MTRB1 that were grown anaerobically with fumarate as the electron acceptor. The specific cytochrome content is the difference between the absorbance at the peak and the absorbance at the trough for the Soret region from reduced-minus-oxidized difference spectra per milligram of protein. The values are means ± standard deviations for results of independent experiments (three independent cultures of each strain). A section sign indicates that the value is statistically significantly different from the value for MR-1 at a P value of <0.001.

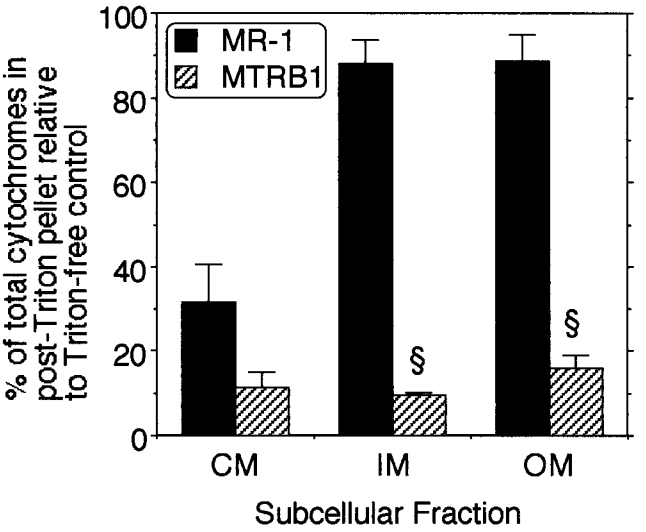

FIG. 6. Ability of 2% Triton X-100 in the presence of 10 mM $MgCl_2$ to solubilize the cytochromes of various membrane fractions isolated from anaerobically grown cells of MR-1 and MTRB1. The Triton X-100-insoluble material was pelleted by ultracentrifugation and analyzed spectrally to determine cytochrome content. The values are the percentages of total cytochromes associated with the post-Triton X-100 pellet relative to the amounts in the Triton X-100-free controls. All values are means ± standard deviations ($n = 2$) for independent subcellular fractions from each strain. A section sign indicates that the value is statistically significantly different from the value for MR-1 at a P value of <0.001.

fractions are largely insoluble (15). As expected, the CM cytochromes of both MR-1 and MTRB1 were markedly solubilized by Triton X-100 (Fig. 6). In contrast to the cytochromes in the CM, approximately 90% of the cytochromes in the IM and OM fractions of MR-1 were resistant to Triton X-100 solubilization; i.e., these cytochromes remained associated with the Triton X-100-insoluble pellet (Fig. 6), which agrees with previous findings (15). The results obtained with MTRB1 were much different; only 10 to 16% of the cytochromes of the IM and OM fractions remained with the post-Triton X-100 pellet (Fig. 6). To determine if the prominent Triton X-100 solubility of the OM cytochromes of MTRB1 could be due to marked contamination of the OM fraction with CM, the distribution of the CM-specific marker NADH oxidase was examined. The NADH oxidase activity of the OM of MTRB1 was 12% that of the CM (data not shown), which is in line with the values previously reported for MR-1 (13 to 15%) (14, 21). The similarity of the SDS-PAGE protein patterns of the OM fractions from MR-1 and MTRB1 (Fig. 5) further support the predominant OM nature of the OM fraction from MTRB1. Together, these findings indicate that the cytochromes associated with the OM and IM fractions of MTRB1 are not anchored tightly to these membranes, as the IM and OM cytochromes of MR-1 are.

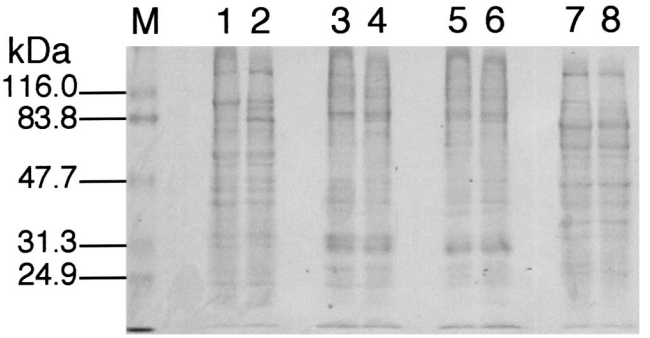

FIG. 5. Pro-Blue-stained SDS-PAGE profiles of subcellular fractions prepared from cells grown anaerobically with fumarate as the electron acceptor. Lanes 1, 3, 5, and 7, MR-1; lanes, 2, 4, 6, and 8, MTRB1. The lanes were loaded with 25 μg of protein from each of the following subcellular fractions: CM (lanes 1 and 2), IM (lanes 3 and 4), OM (lanes 5 and 6), and soluble fraction (lanes 7 and 8). The numbers on the left indicate the migration positions and molecular masses of TriChromRanger prestained protein markers (Pierce) in lane M.

Western blotting with anti-MtrB indicated that MtrB was localized to the IM and OM fractions of MR-1 but was absent from all fractions of MTRB1 (Fig. 7). While MtrB is therefore an OM protein, *mtrB* gene replacement would not likely have interrupted OM cytochrome expression, since the OM cytochrome genes (including *omcA* and *omcB*) are upstream from *mtrB*. Antibodies specific for OmcA and OmcB were used to determine the relative levels and subcellular localization of these proteins in MTRB1 and MR-1. Consistent with previous findings (27, 28), OmcA and OmcB were localized primarily in the OM and IM of MR-1 (Fig. 8). In MTRB1, however, significant amounts of OmcA and OmcB were also detected in the CM (Fig. 8). OmcA and OmcB were also detected in the soluble fraction of MTRB1, but the level of OmcB in the soluble fraction was clearly less than the levels in the membrane subfractions (data not shown). While OmcA and OmcB

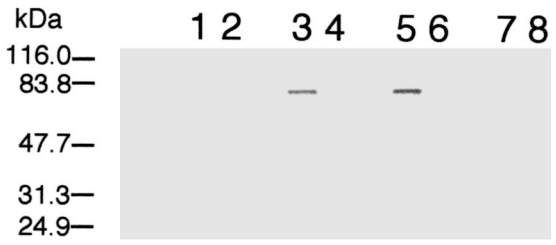

FIG. 7. Western blots obtained by using polyclonal IgG specific for MtrB. The lanes were loaded with 5 μg of protein of each of the following subcellular fractions: CM (lanes 1 and 2), IM (lanes 3 and 4), OM (lanes 5 and 6), and soluble fraction (lanes 7 and 8). The subcellular fractions were prepared from cells grown anaerobically with fumarate as the electron acceptor. Lanes 1, 3, 5, and 7, MR-1; lanes, 2, 4, 6, and 8, MTRB1. The results are representative of the results obtained for two independent cultures of each strain.

in MR-1 are resistant to Triton X-100 solubilization, these proteins in MTRB1 are readily solubilized by Triton X-100, regardless of their subcellular localization (Fig. 8). These findings agree with those obtained for relative Triton X-100 solubilization of total IM and OM cytochromes determined spectrally (Fig. 6). Overall, while MTRB1 still synthesizes OmcA and OmcB, significant amounts of both proteins are mislocalized to the CM. Furthermore, the enhanced Triton X-100 solubility of these OM cytochromes in MTRB1 suggests that they are not properly incorporated into the OM.

The Western blots in Fig. 8 show that OmcA migrated as a single band near the expected mass, 82.7 kDa. In previous Western blots, OmcA appeared as a broad band spanning approximately 83 to 66 kDa, with the greatest intensity at the upper and lower regions (27, 28). In these previous studies, the subcellular fractions were not heated in SDS solubilization mixture before they were loaded on the gels so that direct

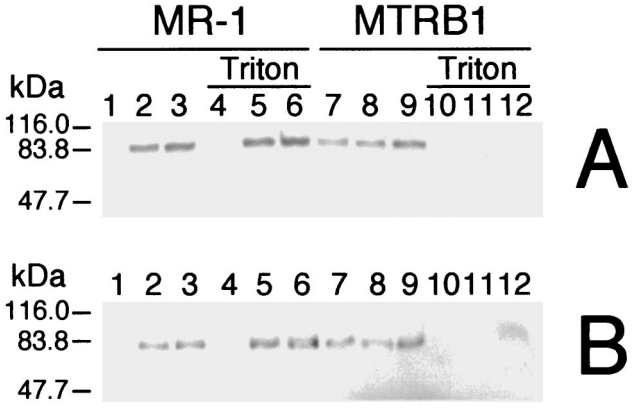

FIG. 8. Western blots obtained by using polyclonal IgG specific for OmcA (A) or OmcB (B). Membrane fractions isolated from fumarate-grown cells of MR-1 (lanes 1 to 6) and MTRB1 (lanes 7 to 12) were treated with 2% Triton X-100–10 mM $MgCl_2$ (lanes 4, 5, 6, 10, 11, and 12) or Triton-free buffer (lanes 1, 2, 3, 7, 8, and 9), after which the insoluble material was pelleted by ultracentrifugation and loaded onto SDS-PAGE gels. The lanes contained samples of the following subcellular fractions: CM (lanes 1, 4, 7, and 10), IM (lanes 2, 5, 8, and 11), and OM (lanes 3, 6, 9, and 12). The results are representative of the results of experiments performed with two independent subcellular fractions from each strain.

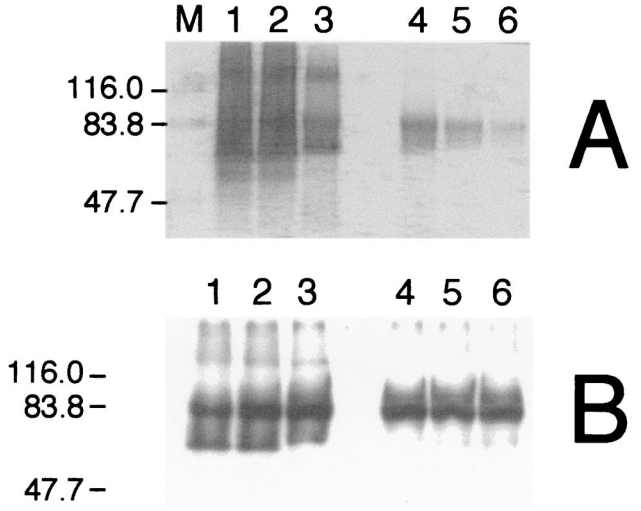

FIG. 9. SDS-PAGE analysis of OM isolated from MR-1 cells grown anaerobically with fumarate. The gel in panel A was stained for heme, while the gel in panel B is a Western blot probed with anti-OmcA. Prior to loading on the gels, each sample (5 μg of OM protein) was incubated for 5 min in SDS solubilization mixture at 22°C (lane 1), 30°C (lane 2), 40°C (lane 3), 50°C (lane 4), 60°C (lane 5), or 70°C (lane 6). The numbers on the left indicate the migration positions and molecular weights of the prestained protein markers in lane M.

comparisons could be made with samples that were analyzed by heme staining. In contrast, the samples in this study (Fig. 7 and 8) were boiled in SDS solubilization mixture for 5 min. The effects of heating the OM samples in SDS solubilization mixture at several temperatures prior to loading of the gel were examined. When samples were solubilized at either room temperature or 30°C, OmcA appeared as a broad band with prominent intensity in the upper and lower regions (Fig. 9B). Some band sharpening occurred at 40°C, and for samples heated at 50 to 70°C most OmcA was confined to a single band at approximately 83 kDa (Fig. 9B). The OmcA bands in Fig. 9 are more intense than those in Fig. 8 because the protein load was approximately five times greater in the gel shown in Fig. 9. These results demonstrate that the higher temperatures used in this study were responsible for the sharpening of the OmcA material to a single species migrating at 83 kDa (Fig. 8).

Higher temperatures also resulted in less smearing in heme-stained gels (Fig. 9A), but they also destroyed much of the heme-positive material. At 50°C, most heme activity was localized at approximately 83 kDa, and a heme-positive smear extended down to approximately 70 kDa (Fig. 9A). OmcB, which migrated at approximately 77 kDa (Fig. 8), was within this range. In previous studies with samples solubilized at room temperature, heme-positive bands representing OmcB were also observed at approximately 53 to 62 kDa (27). While heme-postive material was observed in this 53- to 62-kDa region for samples solubilized at 22 and 30°C, much of it disappeared at 40°C, and all of it disappeared at 50°C (Fig. 9A). Together, these findings suggest that the smearing and apparent lower-molecular-weight forms of OmcA and OmcB are due to incomplete denaturation by SDS at room temperature. Higher temperatures result in more complete denaturation and migration more indicative of the actual mass. It is unlikely that the

apparent lower-molecular-weight forms are the result of partial proteolysis because such smaller fragments would also have been observed in samples solubilized at higher temperatures.

Characterization of the *mtrF* and *mtrF-omcA* mutants. It is possible that the absence of MtrB in MTRB1 might similarly disrupt proper incorporation of the other putative OM cytochrome (MtrF) into the OM. However, antibodies specific for MtrF are not available yet, so the localization of MtrF could not be directly examined. Instead, this issue was addressed functionally by determining if MtrF is necessary for Fe(III) or Mn(IV) reduction. An *mtrF* gene replacement mutant, MTRF1, was isolated. MTRF1 lacked the expected wild-type PCR product (obtained with primers F1 and F2) for *mtrF* but was positive for a PCR product that was ~1.6 kb larger (data not shown), which is consistent with replacement of 0.5 kb of *mtrF* with the ~2.1-kb Km^r gene.

In the event that OmcA could compensate for the absence of MtrF, a double mutant lacking both *mtrF* and *omcA* (MTRF-OMCA) was also isolated by gene replacement. MTRF-OMCA lacked the expected wild-type PCR product (obtained with primers F1 and A2) for *mtrF-omcA* but was positive for a PCR product that was ~0.4 kb smaller (data not shown), which is consistent with replacement of a 2.5-kb *mtrF-omcA* fragment with the ~2.1-kb Km^r gene. MTRF-OMCA lacked the wild-type 1.6-kb PCR product when primers F3 and A4 were used (data not shown); these two primers would have hybridized within the *mtrF-omcA* region that was deleted in MTRF-OMCA. MTRF1 and MTRF-OMCA were both positive for the PCR product (obtained with primer K1) expected for the Km^r gene used to interrupt *mtrF* and *mtrF-omcA*, respectively, but were unable to grow on medium containing chloramphenicol. Overall, these results are consistent with the expected double-crossover gene replacements.

Compared to MR-1, MTRF1 was not deficient in reduction of δMnO_2, Fe(III) citrate, or αFeOOH (Fig. 10). If anything, it exhibited marginally higher rates of Fe(III) reduction than MR-1. While the double mutant MTRF-OMCA was not deficient in Fe(III) reduction, it reduced δMnO_2 at 61% of the rate of MR-1 (Fig. 10B). This finding is similar to a previous finding which showed that a mutant lacking only OmcA reduced Mn(IV) at 55% of the rate of MR-1 (27). The anaerobic growth of MTRF1 and the anaerobic growth of MTRF-OMCA on fumarate and DMSO were very similar to the anaerobic growth of MR-1; i.e., all three strains reached essentially the same maximal culture turbidity after 24 h (data not shown). All three strains also reduced 2 mM nitrate to undetectable levels by 24 h; nitrite was not detected at 24 h, indicating that nitrite was also reduced (data not shown). Overall, loss of MtrF does not affect the use of various electron acceptors, and a mutant that has lost both MtrF and OmcA resembles a previously characterized *omcA* mutant and has a partial deficiency only in Mn(IV) reduction.

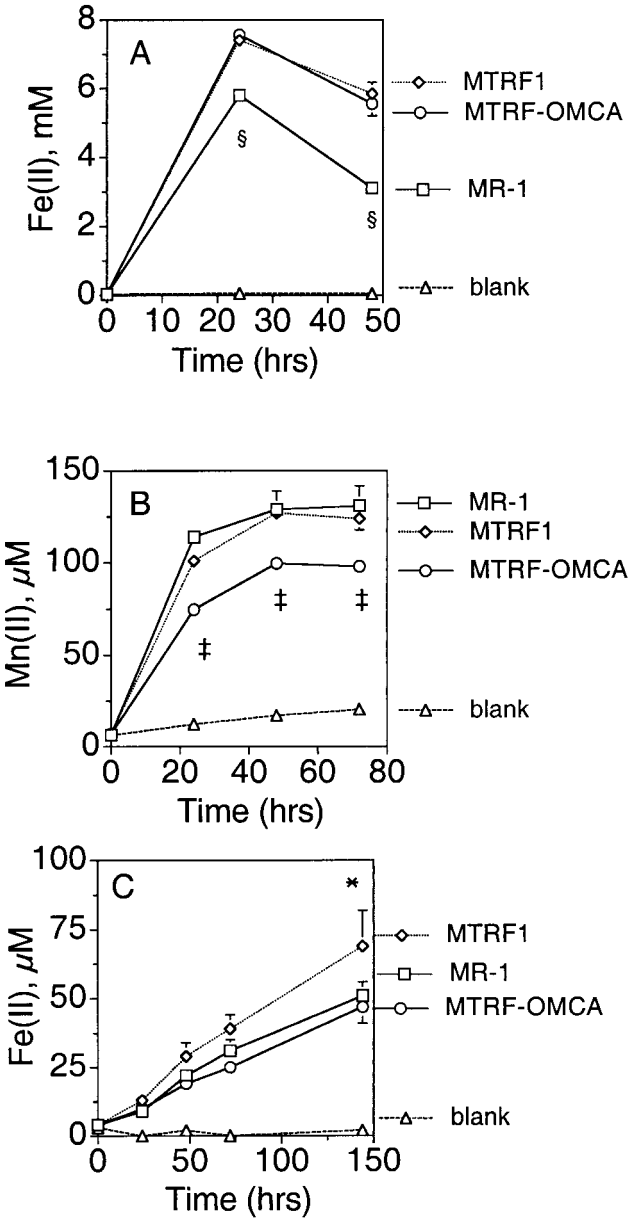

FIG. 10. Reduction of Fe(III) citrate (A), δMnO_2 (B), or αFeOOH (C) by cells of various strains under anaerobic conditions as determined by the formation of Mn(II) or Fe(II) over time. All values are means ± standard deviations for three independent cultures of each strain. For points lacking error bars, the bars were smaller than the symbols. A section sign indicates that the value for MR-1 is significantly different from the values for the other two strains ($P < 0.001$). A double dagger indicates that the value for MTRF-OMCA is significantly different from the values for the other two strains ($P < 0.01$). An asterisk indicates that the value for MTRF1 is significantly different from the values for MR-1 ($P < 0.05$) and MTRF-OMCA ($P < 0.01$).

DISCUSSION

The ability of MR-1 to obtain energy for growth via reduction of insoluble Mn(IV) and Fe(III) oxides under anaerobic conditions implies that there is a mechanism that links the electron transport machinery in the CM to the reduction of these extracellular metal oxides. It has been demonstrated previously that the tetraheme cytochrome CymA, which is associated with the CM, is required for the reduction of Mn(IV) and Fe(III) (20, 26). Similarly, menaquinone is also required for Mn(IV) and Fe(III) reduction by MR-1 (18). While the subcellular location of menaquinone has not been definitely addressed in MR-1, this molecule is presumably associated

with the CM based on evidence from other species. These CM components are likely part of electron transport chains that eventually transfer electrons to redox-active components in the OM. The localization of cytochromes (e.g., OmcA and OmcB) to the OM of anaerobically grown MR-1 (15, 21, 27) suggests a plausible mechanism by which electrons could be transferred to insoluble metal oxides at the cell surface.

The requirement for MtrB for proper localization of OM cytochromes and possibly other OM components has important implications for the ability of MR-1 to reduce extracellular electron acceptors. The results of studies with polynuclear Fe(III) complexes are consistent with Fe(III) reductase activity in the OM (8). Force microscopy demonstrated that the affinity between MR-1 cells and αFeOOH increased up to fivefold under anaerobic conditions, and force curve signatures were consistent with the presence of an Fe(III) reductase in the OM (13).

The majority of formate-dependent Fe(III) reductase activity has been localized to the OM of MR-1 (17), even though the OM fraction contains only small amounts of CM contaminants (e.g., NADH oxidase activity) and formate dehydrogenase (mostly localized to the soluble fraction of MR-1) (17). If instead the Fe(III) reductase were in the CM, the CM would exhibit very prominent rates of Fe(III) reduction because of its CymA and menaquinone contents. The observation that crude membranes from MR-1 exhibit significantly higher rates of Fe(III) reduction (32) than the rates previously reported for CM and OM fractions (17) supports the hypothesis that electron transport components in the CM (e.g., menaquinone and CymA) are likely part of electron transport chains that eventually transfer electrons to metal-reducing components in the OM. Alternatively, the higher Fe(III) reductase activity observed for crude membranes could imply that there are Fe(III) reductases in both the CM and the OM. However, in this case, the sum of the CM and OM activities should equal the activities of the crude membranes, but the crude membrane activity has been reported to be much greater than the sum of the activities (32). While there may be a second Fe(III) reductase in the CM (8, 17), it is unclear if this activity is associated with anaerobic respiration. If there were both CM and OM Fe(III) reductases, they would both have to be downstream of menaquinone and CymA, since the absence of either results in a nearly total loss of Fe(III) reduction by cells (18, 26). The finding that a type II secretion mutant of *S. putrefaciens* strain 200 does not reduce Fe(III) (7) suggests that there is not a prominent dissimilatory Fe(III) reductase in the CM because type II secretion would not predictably be necessary for the localization of CM components. The overall data therefore seem to favor the hypothesis that CM electron transport components supply electrons to OM reductases.

The prominent deficiency in Mn(IV) and Fe(III) reduction by MTRB1 is consistent with the findings obtained for SR-21, an *mtrB* mutant isolated by transposon mutagenesis, although SR-21's deficiency in Mn(IV) reduction was assessed only qualitatively (2). SR-21 was isolated from MR-1R, a rifampin-resistant mutant, but was compared to MR-1 and not to its parent, MR-1R (2). Two other independently isolated rifampin-resistant mutants of MR-1 have markedly depressed levels of menaquinone and are considerably slower than MR-1 at utilizing electron acceptors that require menaquinone (26), including Mn(IV) and Fe(III). It is therefore possible that the differences in Mn(IV) and Fe(III) reduction between SR-21 and MR-1R are smaller than those between SR-21 and MR-1.

Including the mutant described in this report, three *mtrB* mutants have been described, and all of them exhibit deficiencies in Mn(IV) and Fe(III) reduction. However, the different methods used to construct the mutations could conceivably have resulted in some differences between the strains. MTRB1 was isolated by gene replacement. In contrast, AQ-38 and SR-21 were isolated by mini-Tn*10* and Tn*5* mutagenesis, respectively, with the sites determined by sequencing DNA flanking one end of the transposon (2, 35). While Tn*5*-based systems are supposed to mediate simple insertions, a large (9- to 11-kb) genomic deletion has been reported with Tn*phoA* (derived from Tn*5*) mutagenesis of MR-1, such that the flanking DNA did not define the gene that was critical to the phenotype (T. M. Mertins, J. M. Myers, and C. R. Myers, Abstr. 100th Gen. Meet. Am. Soc. Microbiol., abstr. H-11, 2000). The reported characterization of SR-21 was not sufficient to rule out such deletions or other unexpected events.

The lack of obvious electron transport moieties in MtrB makes the role of this protein in metal reduction unclear. Because MtrB contains a postulated metal-binding site (CXXC), it has been proposed that this protein may have a role in metal binding during reduction (2). However, there is no evidence to substantiate the hypothesis that this site plays this role in MtrB. In a partial search of the MR-1 genome for open reading frames that might encode CXXC, more than 80 such sites were found exclusive of the CXXCH heme *c*-binding sites. It is doubtful that all of these sites are metal-binding sites. The hypothesis that CXXC sequences serve as metal-binding sites likely originated with metallothioneins, in which such domains bind Cd^{2+}, Zn^{2+}, or Cu^{2+} (31). The chemistry of these metals is very different from that of Fe(III) and Mn(IV). Furthermore, the role of MtrB is not limited to metal reduction. In addition to being unable to reduce MnO_2 and $Fe(OH)_3$, *mtrB* mutant AQ-38 is also unable to reduce 10 mM anthraquinone-2,6-disulfonate (AQDS) (35), a putative shuttle for extracellular electron transfer. The role of a metal-binding site in MtrB in AQDS reduction is not clear.

The findings described in this report provide a more plausible role for MtrB in metal reduction, namely, that it is required for proper incorporation of cytochromes into the OM. Not only were significant amounts of OmcA and OmcB mislocalized to the CM (Fig. 9), but the OmcA and OmcB proteins that were in the OM of MTRB1 were not properly inserted into the OM (Fig. 6 and 8). The attachment of heme *c* groups to the OmcA and OmcB apoproteins may have also been affected. This is likely true for the populations of OmcA and OmcB that were mislocalized to the CM, because a spectral increase in total cytochrome content was not detected in the CM of MTRB1 (Fig. 4). Since heme *c* binding occurs on the periplasmic face of the CM (38), improper translocation across the CM could diminish heme *c* attachment.

The inability of MTRB1 to properly insert OmcA and OmcB into the OM has direct implications for Mn(IV) reduction because these proteins have a role in Mn(IV) reduction (3, 27). While OmcB (MtrC) may contribute to Fe(III) reduction, it is not clear that it is required (3, 27, 28). The possibility that MtrB may also influence the proper localization and/or inser-

tion of other OM proteins must be considered. For example, the requirement for MtrB for AQDS reduction (35) may indicate that MtrB has a role in the incorporation of AQDS-reducing components into the OM. While we could not determine if MtrB was required for proper localization of another putative OM cytochrome (MtrF), improper localization of MtrF would probably not affect the ability to reduce Mn(IV) and Fe(III) because an *mtrF* mutant was not compromised in terms of its ability to reduce these metals (Fig. 10).

Exactly how MtrB might influence the localization and/or insertion of OM proteins is not known at this time. One possibility is that MtrB acts as some sort of chaperone. The mislocalization of OmcA and OmcB to the CM in the *mtrB* mutant MTRB1 resembles findings obtained with a type II secretion mutant of *S. putrefaciens* strain 200 (7). A 91-kDa heme-containing protein which is apparently localized to the outer face of the OM in strain 200 was not surface associated in the type II mutant and was at least partially mislocalized to the CM (7). However, *mtrB* is not homologous to known type II secretion genes, and *mtrB* is not part of the multigene cluster encoding the type II secretion system in MR-1.

On the basis of Sarkosyl insolubility, MtrB was postulated to be an OM protein (2). The degree to which the Sarkosyl method distinguishes between CM and OM components in MR-1 was not determined. However, the subcellular fractionation method used in this study, for which the distribution of various markers is well documented (14–18, 20, 21), supports an OM localization for MtrB (Fig. 7). Since MtrB is not associated with the CM, it probably does not translocate proteins across the CM. It could, however, facilitate the transfer of proteins to the OM once they are exposed on the outer face of the CM. Another possibility is that MtrB is a critical component of a multiprotein complex that properly anchors or orients certain proteins in the OM. The high degree of heme-positive smearing in OM exposed to SDS at 22 to 30°C (Fig. 9) suggests that there are multiprotein cytochrome-containing complexes that are not easily dissociated by SDS. In addition, a high-molecular-weight heme-positive band (ca. 150 kDa) was found in samples treated with SDS at 22 to 40°C but was absent in samples treated at higher temperatures. While this ~150-kDa band has been consistently obtained with OM fractions solubilized in SDS at room temperature (21, 25), our analysis of the MR-1 genomic sequence to date has not identified a *c*-type cytochrome with this high molecular weight. Together, these observations suggest that the ~150-kDa band may represent a multiprotein complex that requires SDS at higher temperatures to facilitate dissociation.

When transposon mutagenesis was used to generate an *omcB* (*mtrC*) mutant, the transposon exerted polar effects which blocked the expression of the downstream genes *mtrA* and *mtrB*, suggesting that *omcB*, *mtrA*, and *mtrB* are transcribed as a polycistronic mRNA (3). In contrast, reverse transcription-PCR indicated that the *mtrA* and *mtrB* genes are expressed in an *omcB* mutant (OMCB1) generated by gene replacement (27). OMCB1 exhibited much greater rates of Fe(III) citrate reduction than MTRB1 exhibited. For example, OMCB1 generated >2 mM Fe(II) after 3 days, whereas MTRB1 generated only 0.38 mM Fe(II). The differences in Fe(III) citrate reduction between OMCB1 and MTRB1 were statistically significant after 1 day ($P < 0.05$) and after 2 and 3 days ($P < 0.001$). The continued expression of at least some MtrB by OMCB1 likely contributes to its higher rates of Fe(III) citrate reduction and implies that MtrB has a critical role in the localization of at least one component necessary for Fe(III) reduction.

In summary, the absence of MtrB resulted in a prominent decline in the specific cytochrome content of the OM, with mislocalization of significant amounts of OmcA and OmcB to the CM. The inability of the *mtrB* mutant to properly insert these, and possibly other, proteins into its OM likely contributes to its marked deficiency in Mn(IV) and Fe(III) reduction. Therefore, the contribution of MtrB to the use of extracellular electron acceptors is likely indirect; i.e., MtrB is required for the proper incorporation of electron transport components into the OM.

ACKNOWLEDGMENTS

This work was supported by National Institute of Health grant R01GM50786 to C.R.M. We are also grateful for the support of the STRATTEC Foundation.

The preliminary genomic sequence data were obtained from The Institute for Genomic Research through a website (http://www.tigr.org). Sequencing of *S. putrefaciens* MR-1 genomic DNA by The Institute for Genomic Research was accomplished with support from the Department of Energy.

REFERENCES

1. **Armstrong, P. B., W. B. Lyons, and H. E. Gaudette.** 1979. Application of formaldoxime colorimetric method for the determination of manganese in the pore water of anoxic estuarine sediments. Estuaries **2:**198–201.
2. **Beliaev, A. S., and D. A. Saffarini.** 1998. *Shewanella putrefaciens mtrB* encodes an outer membrane protein required for Fe(III) and Mn(IV) reduction. J. Bacteriol. **180:**6292–6297.
3. **Beliaev, A. S., D. A. Saffarini, J. L. McLaughlin, and D. Hunnicutt.** 2001. MtrC, an outer membrane decahaem *c* cytochrome required for metal reduction in *Shewanella putrefaciens* MR-1. Mol. Microbiol. **39:**722–730.
4. **Brewer, P. G., and D. W. Spencer.** 1971. Colorimetric determination of manganese in anoxic waters. Limnol. Oceanogr. **16:**107–110.
5. **Cataldo, D. A., M. Haroon, L. E. Schrader, and V. L. Youngs.** 1975. Rapid colorimetric determination of nitrate in plant tissue by nitration of salicylic acid. Commun. Soil Sci. Plant Anal. **6:**71–80.
6. **de Lorenzo, V., M. Herrero, U. Jakubzik, and K. N. Timmis.** 1990. Mini-Tn*5* transposon derivatives for insertional mutagenesis, promoter probing, and chromosomal insertion of cloned DNA in gram-negative eubacteria. J. Bacteriol. **172:**6568–6572.
7. **DiChristina, T. J., C. M. Moore, and C. A. Haller.** 2002. Dissimilatory Fe(III) and Mn(IV) reduction by *Shewanella putrefaciens* requires *ferE*, a homolog of the *pulE* (*gspE*) type II protein secretion gene. J. Bacteriol. **184:**142–151.
8. **Dobbin, P. S., L. M. Requena Burmesiter, S. L. Heath, A. K. Powell, A. G. McEwan, and D. J. Richardson.** 1996. The influence of chelating agents upon the dissimilatory reduction of Fe(III) by *Shewanella putrefaciens*. Part 2. Oxo- and hydroxo-bridged polynuclear Fe(III) complexes. BioMetals **9:**291–301.
9. **Hayashi, S., and H. C. Wu.** 1990. Lipoproteins in bacteria. J. Bioenerg. Biomembr. **22:**451–471.
10. **Hoyle, B., and T. J. Beveridge.** 1983. Binding of metallic ions to the outer membrane of *Escherichia coli*. Appl. Environ. Microbiol. **46:**749–752.
11. **Kinder, S. A., J. L. Badger, G. O. Bryant, J. C. Pepe, and V. L. Miller.** 1993. Cloning of the *Yen*I restriction endonuclease and methyltransferase from *Yersinia enterocolitica* serotype O8 and construction of a transformable R^-M^+ mutant. Gene **136:**271–275.
12. **Lovley, D. R., and E. J. P. Phillips.** 1986. Organic matter mineralization with reduction of ferric iron in anaerobic sediments. Appl. Environ. Microbiol. **51:**683–689.
13. **Lower, S. K., M. F. J. Hochella, and T. J. Beveridge.** 2001. Bacterial recognition of mineral surfaces: nanoscale interactions between *Shewanella* and α-FeOOH. Science **292:**1360–1363.
14. **Myers, C. R., B. P. Carstens, W. E. Antholine, and J. M. Myers.** 2000. Chromium(VI) reductase activity is associated with the cytoplasmic membrane of anaerobically grown *Shewanella putrefaciens* MR-1. J. Appl. Microbiol. **88:**98–106.
15. **Myers, C. R., and J. M. Myers.** 1992. Localization of cytochromes to the outer membrane of anaerobically grown *Shewanella putrefaciens* MR-1. J. Bacteriol. **174:**3429–3438.

16. **Myers, C. R., and J. M. Myers.** 1992. Fumarate reductase is a soluble enzyme in anaerobically grown *Shewanella putrefaciens* MR-1. FEMS Microbiol. Lett. **98:**13–20.
17. **Myers, C. R., and J. M. Myers.** 1993. Ferric reductase is associated with the membranes of anaerobically grown *Shewanella putrefaciens* MR-1. FEMS Microbiol. Lett. **108:**15–22.
18. **Myers, C. R., and J. M. Myers.** 1993. Role of menaquinone in the reduction of fumarate, nitrate, iron(III) and manganese(IV) by *Shewanella putrefaciens* MR-1. FEMS Microbiol. Lett. **114:**215–222.
19. **Myers, C. R., and J. M. Myers.** 1994. Ferric iron reduction-linked growth yields of *Shewanella putrefaciens* MR-1. J. Appl. Bacteriol. **76:**253–258.
20. **Myers, C. R., and J. M. Myers.** 1997. Cloning and sequence of *cymA*, a gene encoding a tetraheme cytochrome *c* required for reduction of iron(III), fumarate, and nitrate by *Shewanella putrefaciens* MR-1. J. Bacteriol. **179:** 1143–1152.
21. **Myers, C. R., and J. M. Myers.** 1997. Outer membrane cytochromes of *Shewanella putrefaciens* MR-1: spectral analysis, and purification of the 83-kDa c-type cytochrome. Biochim. Biophys. Acta **1326:**307–318.
22. **Myers, C. R., and K. H. Nealson.** 1988. Microbial reduction of manganese oxides: interactions with iron and sulfur. Geochim. Cosmochim. Acta **52:** 2727–2732.
23. **Myers, C. R., and K. H. Nealson.** 1988. Bacterial manganese reduction and growth with manganese oxide as the sole electron acceptor. Science **240:** 1319–1321.
24. **Myers, C. R., and K. H. Nealson.** 1990. Respiration-linked proton translocation coupled to anaerobic reduction of manganese(IV) and iron(III) in *Shewanella putrefaciens* MR-1. J. Bacteriol. **172:**6232–6238.
25. **Myers, J. M., and C. R. Myers.** 1998. Isolation and sequence of *omcA*, a gene encoding a decaheme outer membrane cytochrome *c* of *Shewanella putrefaciens* MR-1, and detection of *omcA* homologs in other strains of *S. putrefaciens*. Biochim. Biophys. Acta **1373:**237–251.
26. **Myers, J. M., and C. R. Myers.** 2000. Role of the tetraheme cytochrome CymA in anaerobic electron transport in cells of *Shewanella putrefaciens* MR-1 with normal levels of menaquinone. J. Bacteriol. **182:**67–75.
27. **Myers, J. M., and C. R. Myers.** 2001. Role for outer membrane cytochromes OmcA and OmcB of *Shewanella putrefaciens* MR-1 in reduction of manganese dioxide. Appl. Environ. Microbiol. **67:**260–269.
28. **Myers, J. M., and C. R. Myers.** 2002. Genetic complementation of an outer membrane cytochrome *omcB* mutant of *Shewanella putrefaciens* MR-1 requires *omcB* plus downstream DNA. Appl. Environ. Microbiol. **68:**2781–2793.
29. **Ochman, H., A. S. Gerber, and D. L. Hartl.** 1988. Genetic applications of an inverse polymerase chain reaction. Genetics **120:**621–623.
30. **Osborn, M. J., J. E. Gander, E. Parisi, and J. Carson.** 1972. Mechanism of assembly of the outer membrane of *Salmonella typhimurium*: isolation and characterization of cytoplasmic and outer membrane. J. Biol. Chem. **247:** 3962–3972.
31. **Petering, D. H., M. Dughish, M. Huang, S. Krezoski, S. Krull, D. Lewand, A. Muñoz, L. Ren, S. Venkatest, S. Blumenthal, and C. F. Shaw III.** 1998. Cellular metallothionein: properties of apometallothionein and the comparative toxicity of Cd^{2+} and Cd-metallothionein, p. 459–468. *In* Metallothionein IV. Birkh¨auser Verlag, Basal, Switzerland.
32. **Saffarini, D. A., S. L. Blumerman, and K. J. Mansoorabadi.** 2002. Role of menaquinones in Fe(III) reduction by membrane fractions of *Shewanella putrefaciens*. J. Bacteriol. **184:**846–848.
33. **Sambrook, J., E. F. Fritsch, and T. Maniatis.** 1989. Molecular cloning: a laboratory manual, 2nd ed. Cold Spring Harbor Laboratory, Cold Spring Harbor, N.Y.
34. **Schnaitman, C. A.** 1971. Solubilization of the cytoplasmic membrane of *Escherichia coli* by Triton X-100. J. Bacteriol. **108:**545–552.
35. **Shyu, J. B. H., D. P. Lies, and D. K. Newman.** 2002. Protective role of *tolC* in efflux of the electron shuttle anthraquinone-2,6-disulfonate. J. Bacteriol. **184:**1806–1810.
36. **Simon, R., U. Priefer, and A. Pühler.** 1983. A broad host-range mobilization system for in vivo genetic engineering: transposon mutagenesis in Gram-negative bacteria. Bio/Technology **1:**37–45.
37. **Thomas, P. E., D. Ryan, and W. Levin.** 1976. An improved staining procedure for the detection of the peroxidase activity of cytochrome P-450 on sodium dodecyl sulfate polyacrylamide gels. Anal. Biochem. **75:**168–176.
38. **Thöny-Meyer, L.** 1997. Biogenesis of respiratory cytochromes in bacteria. Microbiol. Mol. Biol. Rev. **61:**337–376.
39. **van'T Riet, J., A. H. Stouthamer, and R. J. Planta.** 1968. Regulation of nitrate assimilation and nitrate respiration in *Aerobacter aerogenes*. J. Bacteriol. **96:**1455–1464.